Shock-Fitting Applied to Relaxation Solutions of Transonic Small-Disturbance Equations

Mohammed M. Hafez* and H. K. Cheng†
University of Southern California, Los Angeles, Calif.

Shock-fitting is applied to relaxation solutions of transonic small-disturbance equations. Finite-difference algorithms expressing conservation laws across the discontinuity are introduced in a manner consistent with the type-sensitive difference schemes of Murman and Cole. Results are presented for flows involving embedded as well as bow shocks. Comparison with shock-capturing solutions based on the shock-point operator (SPO) is made for the same grid with comparable computation time. Substantial improvement in accuracy by the shock-fitting is demonstrated for mesh size in the range of practical interest. The iteration convergence of shock-fitting solutions can also be improved with the use of acceleration algorithms based on the power method; a savings in computer time of a factor of four is demonstrated.

I. Introduction

THIS paper presents a study of shock-fitting applied to relaxation solutions for the transonic small-disturbance equation, in which the shock is treated as a surface of discontinuity. Shock-fitting for finite-difference solutions to the inviscid compressible flow problem has been carried out in the past mostly in the framework of an unsteady flow.[1,2,3] The steady flow solution of interest can be recovered as a limit of the time-dependent solutions; but, this proves to be far more costly than the relaxation methods (for time-dependent methods with shock-capturing, see Refs. 4 and 5).

In the line-relaxation method based on type-sensitive difference schemes introduced by Murman and Cole,[6] the shock is captured as a part of the continuous solution (owing largely to the numerical viscosity introduced by the difference schemes), and is smeared out over several grid points. Solutions following the procedure of Ref. 6 have been known to give grossly inaccurate shock jumps; they also disagree with the shock solutions arrived through the time-dependent approach.[4,5] More seriously is, perhaps, the fact that these discrepancies do not vanish with grid refinement, as confirmed by Murman in Ref. 7. The remedy proposed by Murman for his otherwise powerful and widely adopted procedure turns out to be attractively simple; it involves mainly the replacement of the elliptic difference operator near the transition curve by a modified one, referred to as the "shock-point operator (SPO)."[7] However, the SPO solution, as well as its more recent adaptions to other transonic computer programs (Refs. 8 and 9), still require four or more grid points to complete a shock jump. Essential to the present study is the observation that SPO in the form of Refs. 7-9 reduces to the ordinary hyperbolic difference operator whereever the downstream flow is supersonic. Therefore, SPO cannot improve the Murman-Cole[6] solution in this case (which is known to yield a rather poor description of a supersonic-supersonic shock transition). More important is, perhaps, the observation that good accuracy of methods using SPO has been fully demonstrated only for one single case,[7] which employs an exceedingly fine grid (500 grid points over a half chord). It is pertinent, therefore, to examine if the alternative, namely, the shock-fitting, may succeed with a *coarser* grid. We will demonstrate that in the range of mesh size of practical interest, shock-fitting does represent an improvement over the shock-capturing (with and without the SPO).

It is noted, however, that the finite-difference solution with shock-fitting may not necessarily represent an improvement over the solution obtained from the original Murman and Cole procedure, unless the re-expansion singularity of Oswatitsch and Zierep[10] is properly accounted for. Subsequent studies show, nevertheless, that this singularity is essentially reproduced without using excessively refined grids.

Aside from the special treatment of the difference operator at a shock point, the treatment of certain neighboring points and other program implementations are equally important. Just as the type-sensitive difference operators are crucial for relaxation solutions for the mixed flows, a distinction between supersonic and subsonic flows behind the shock proves to be also essential in formulating the shock jump condition in difference form, a fact which reflects once again the rule of forbidden signals.

Shock-fitting has the advantage of producing a sharp shock on a coarse grid, while shock-capturing techniques need a very fine mesh to produce a sharp shock, resulting in a prohibitively long computation time. This advantage is gained at the cost of increased complexity in the programming, but this does not appreciably increase the computer work (per sweep) for the program under study. With the larger mesh, one may therefore anticipate a greater savings in the total computer time. Efficient application of shock-fitting to relaxation solutions based on the full potential equation such as Ref. 9 remains a possibility. Relaxation solutions with shock-fitting have also been studied recently by Yu and Seebass in Ref. 11. Their method is applicable only to cases with an imbedded shock with a subsonic downstream and appears to be more complex. A shock problem involving purely supersonic flow was also treated therein using, however, the characteristic method.

This work may be considered as a sequel to another paper, Ref. 12, which studies convergence acceleration of relaxation solutions for transonic flows. The material of the present paper has been drawn mostly from Part II of the University of Southern California Report, USCAE 132,[13] which supersedes AIAA Paper 75-51. Some parts of the presentation have been revised to improve clarity.

The following section provides the transonic small-disturbance equations and associated shock relations, which define the framework for the present study. To facilitate subsequent discussions, the basic difference operators, the related SPO, and some of their relevant properties will be

Presented as Paper 75-51 at the AIAA 13th Aerospace Science Meeting, Pasadena, Calif., Jan. 20-22, 1975; submitted Sept. 2, 1975; revision received Dec. 28, 1976.

Index category: Subsonic and Transonic Flow.

*Research Associate, Department of Aerospace Engineering, Present address: Flow Research, Inc., Kent, Wash. 98031.

†Professor, Department of Aerospace Engineering. Member AIAA.

reviewed. The procedure for shock-fitting is presented in Sec. III. Examples of transonic flow calculations with shock fitting and with SPO are compared and discussed in Sec. IV.

II. The Basic Equations and Preliminary Remarks

We confine the present study of shock-fitting to solutions of the steady transonic small-disturbance theory. The governing partial differential equations (PDE), the boundary conditions, as well as the basic line relaxation program are the same used in our work on convergence acceleration,[12,13] and differ little from those in the original work of Murman and Cole.[6]

A. Equations Governing the Flow Interior and the Shock

In the reduced Cartesian variables x and y, the reduced perturbation velocity potential ϕ satisfies the PDE

$$(K_c-(\gamma+1)\phi_x)\phi_{xx}+\phi_{yy}=0 \tag{1}$$

in an infinite domain. The upper and lower wing boundary conditions are prescribed on a portion of the x-axis as

$$\phi_y=Y'_{\pm}(x) \quad \text{at} \quad |x|<1, \quad y\to 0 \tag{2}$$

The velocity perturbation is required to vanish at the infinity. In the above, γ is the specific heat ratio, and K_c is a transonic similarity parameter. Readers may refer to Refs. 12 and 13 for precise definitions of x,y,ϕ, and K_c, which are not required for the present purpose. (Throughout this paper, the curly bars over x, y and ϕ of Refs. 12 and 13 have been dropped). For a subsonic freestream ($K_c>0$), this solution admits a farfield behavior determined principally by a vortex, doublets and other singularities.‡ This has been applied at a controlled surface to replace the condition at the infinity for the computer solutions in Refs. 6, 12, and 13.

The shock jump relations, consistent with the transonic small-disturbance theory are

$$\langle -K_c+(\gamma+1)\phi_x\rangle=[\![\phi_y]\!]^2/[\![\phi_x]\!]^2 \tag{3}$$

$$[\![\phi_y]\!]/[\![\phi_x]\!]=-\mathrm{d}x^D/\mathrm{d}y \tag{4}$$

where $x=x^D(y)$ represents the shock boundary; $[\![\ ]\!]$ indicates the difference and $\langle\ \rangle$ indicates the average between two values across a discontinuity. Equation (3) may be easily identified with the hodograph shock polar. Equation (4) signifies the continuity of the tangential velocity component, and is equivalent to the continuity of ϕ. Thus, the "ridge," where the potential surfaces in front and behind the shock meet locates the shock boundary. There is a great simplification in the form of the shock polar equation under the transonic small-disturbance theory. Let

$$\hat{u}\equiv(\gamma+1)\ [\![\phi_x]\!]/|K_c-(\gamma+1)\phi_x^-|$$

$$\hat{v}=(3)^{3/2}(\gamma+1)\,|[\![\phi_y]\!]|/4|K_c-(\gamma+1)\phi_x^-|^{3/2} \tag{5}$$

where the superscript "$-$" refers to the preshock condition. Equation (3) then yields the shock polar as a single curve[7]

$$(2+\hat{u})\hat{u}^2=(32/27)\hat{v}^2 \tag{6}$$

B. The Flow Behavior Next to a Shock Root

The shock jump condition takes on a special form in approaching a solid wall, where a singularity causing a local reexpansion appears. Its properties provide an additional theoretical basis for assessing the numerical methods. On a smooth airfoil surface the impermeability condition, Eq. (2), requires a continuous transverse velocity across the shock, hence, the jump relation Eq. (3) reduces to that for a normal shock

$$\langle K_c-(\gamma+1)\phi_x\rangle=0, \quad \text{i.e.,} \quad \langle c_p\rangle=C_p^* \tag{7}$$

Thus, the critical pressure coefficient C_p^* must lie midway between the surface C_p's right in front and right behind the shock.

The singular behavior of the flowfield behind the shock root was uncovered by Oswatitsch and Zierip,[10] following a study by Ackeret, Feldman, and Rott[15] (see also Ref. 16, pg. 355). Physically, the rapid expansion characterized by the singularity arises from a mismatch of the surface streamline curvature with that determined by the shock polar. As such, it represents an interaction of the shock with the subsonic flow, and can be derived from the linearized subsonic equation, using Eqs. (3) and (4) as upstream boundary conditions. Let, $R_0\equiv-[Y''(x_0)]^{-1}$,

$$\xi\equiv(x-x_0)/|(\gamma+1)2^{-1}[\![\phi_{x_0}]\!]^3|^{1/2}R_0, \quad \eta\equiv y/|[\![\phi_{x_0}]\!]|R_0 \tag{8}$$

with the subscript "0" referring to the shock root. The streamwise velocity perturbation and the shock shape near the root can be expressed as functions of ξ and η

$$(\phi_x-(\phi_x^+)_0)/[\![\phi_x]\!]_0\sim 4\pi^{-1}\xi\ln|\zeta/\kappa|+\eta(1-4\pi^{-1}\text{avg}\ \zeta), \tag{9}$$

$$\xi^D\sim 2\pi^{-1}\eta^2[\ln(\eta/\kappa)-\tfrac{1}{2}$$

$$-4^{-1}\pi R_0|(\gamma+1)2^{-1}[\![\phi_x]\!]|^{1/2}(\phi_{xx}^-)_0] \tag{10}$$

where $\zeta=\xi+i\eta$ and the superscripts "$+$" and "$-$" refer once again to the post-shock and preshock conditions, respectively. The parameter κ is an arbitrary constant to be determined by the full solution, but it fixes the position for the maximum surface speed behind the shock at $\xi=\kappa/e$.§ This singularity causes an error of the order $\Delta x/(x-x_0)$ in ϕ_{xx} (hence, in the difference equation) which may not affect, however, the validity of the difference quotient ϕ_x.

C. Shock-Capturing and SPO

As an improvement of the original line-relaxation method of Ref. 6 in shock-capturing, Murman replaces the elliptic difference operator at a supersonic-subsonic transition point by the *shock-point operator*,[7] in which the original x-difference operator is replaced by the sum of the x-differences in an elliptic and a hyperbolic operator. Following essentially Jameson,[9] the difference operators of Refs. 6 and 7 may be more conveniently represented with the introduction of¶

$$U_{ij}\equiv K_c-\frac{(\gamma+1)}{2}\left[\frac{\phi_{i+1,j}-\phi_{ij}}{\Delta x_i}+\frac{\phi_{ij}-\phi_{i-1,j}}{\Delta x_{i-1}}\right]$$

$$P_{ij}\equiv U_{ij}\frac{2}{\Delta x_{i-1}+\Delta x_i}\left[\frac{\phi_{i+1,j}-\phi_{ij}}{\Delta x_i}-\frac{\phi_{ij}-\phi_{i-1,j}}{\Delta x_{i-1}}\right]$$

$$Q_{ij}\equiv\frac{2}{\Delta y_{j-1}+\Delta y_j}\left[\frac{\phi_{i,j+1}-\phi_{ij}}{\Delta y_j}-\frac{\phi_{ij}-\phi_{i,j-1}}{\Delta y_{j-1}}\right]$$

Identifying i and j with the grid position in x and y, the basic difference equations in Murman and Cole's original

‡In the case with lift, other singularities contributed by the nonlinearity are also important. These have been given in part in Cole's 1975 review.[14] With a nonvanishing lift, the potential will be discontinuous, but flow velocities are required to remain continuous everywhere, except across the wing, satisfying also the Kutta condition at $x=1$.

§The shock shape, Eq. (10), derived here appears to be quite different from $\xi^D\propto\eta^{3/2}$ given in Eq. (44) of Ref. 16.

¶P_{ij} may also be expressed as

$$P_{ij}=2\{K_c[(\phi_x)_{i+1/2}-(\phi_x)_{i-1/2}]$$

$$-(\gamma+1)2^{-1}[(\phi_x^2)_{i+1/2}-(\phi_x^2)_{i-1/2}]\}/[\Delta x_{i-1}+\Delta x_i]$$

procedure[6] can be written for variable meshes and to first-order accuracy, as

$$P_{ij}+Q_{ij}-\mu_{ij}(P_{ij}-P_{i-1,j})=0 \tag{11}$$

where μ_{ij} is the switching function which is zero in the elliptic region ($U_{ij}>0$) and unity in the hyperbolic region ($U_{ij}<0$). Jameson interprets Murman's procedure of Ref. 7 simply as a change of $\mu_{ij}\ P_{i-1,j}$ to $\mu_{i-1,j}\ P_{i-1,j}$, i.e., putting the artifical viscosity term into a "conservative form." Namely,

$$P_{ij}+Q_{ij}-\mu_{ij}P_{ij}+\mu_{i-1,j}\ P_{i-1,j}=0 \tag{12}$$

This yields four difference operators corresponding to the elliptic, hyperbolic, parabolic, and the shock points. The parabolic point with $Q_{ij}=0$ occurs next to, and downstream of, the sonic point under acceleration. The "shock point" refers to the grid point next to, and downstream of, the "sonic point" ($U_{ij}=0$) under the flow deceleration; Eq. (12) yields for this point**

$$P_{ij}+P_{i-1,j}+Q_{ij}=0 \tag{13}$$

which is Murman's shock-point operator (SPO).

For a shock which is *plane* and *normal* to the freestream, $Q_{ij}\equiv 0$ and Eq. (13) reproduces correctly the normal shock condition. In general, Eq. (13) cannot yield the correct shock jump which may, nevertheless, be completed in a few (say four or more) steps in Δx through numerical viscosity. The SPO is sensible in that it allows a smooth flow deceleration through the sonic point, where U_{ij} and $U_{i+1,j}$ are of the order Δx and Eq. (13) becomes $Q_{ij}=0(\Delta x)$. However, the procedure according to Eq. (12) yields a hyperbolic operator wherever $U_{ij}<0$ and, therefore, it does not represent an improvement over the original shock-capturing method for treating the shock with a supersonic downstream.

Solutions based on Eq. (12) have been referred to in Refs. 7-9 as being "fully conservative." We shall refer them here as SPO relaxation solutions, or simply SPO solutions. As an algorithm for capturing an embedded shock via line relaxation methods, the SPO proves to be effective in reducing the excessive shock thickness and the error in shock jump.[7-9] However, except for one example utilizing an exceedingly fine grid in Ref. 7, none of the existing SPO solutions can reproduce the shock jump of Eq. (7) with good accuracy (say 3%). Whereas, a bow shock can be located quite adequately by the SPO solution, the portion of the shock with a supersonic downstream takes typically 6-8 grid points to complete the jump (cf. Fig. 3a of Ref. 7).

In the next section, a shock-fitting procedure is introduced which is not limited by the shock inclination and by the stipulation of a subsonic downstream.

III. Shock-Fitting Applied to Line-Relaxation Solutions

Application of shock-fitting to the line relaxation method requires a number of modifications and implementations which are discussed below.

A. Treatment of Points Near Shock

To be consistent with the type-sensitive difference scheme, application of shock-fitting must distinguish the (part of the) shock with a supersonic downstream from that with a subsonic downstream.

1) *Shock with Subsonic Downstream*

Modifications of the difference equations are needed mainly in the treatment of the grid point P next to and downstream of the shock, and a neighboring point Q above or below P belonging to the other side of the shock. Three types of shock inclination must be distinguished, depending on where the shock crosses the vertical through P: 1) a point between P and the next grid point below it, i.e., a forward inclination; 2) a point between P and the next grid point above it, i.e. a backward inclination; 3) a point beyond the two nearest grid points. The inclination in 3) can be either forward or backward and includes the locally normal shock. Figure 1 gives examples typical of these three types.

At point P, which may be referred to as the "shock point," the difference equation in the original line-relaxation procedure is replaced by the first shock-jump equation [Eq. (3)] in the difference form; ϕ_x's are evaluated from central differences at points A and B, and the ϕ_y's from central differences at D and C, in the manner shown in a), b) and c) of Fig. 1. Identifying the shock point P with the grid point (i,j), this difference equation can be written for shocks with a forward inclination (cf. Fig. 1a) as

$$-K_c+\frac{\gamma+1}{2}\left(\frac{\phi_{i-1,j}-\phi_{i-2,j}}{\Delta x_{j-2}}+\frac{\phi_{i+1,j}-\phi_{ij}}{\Delta x_i}\right)$$
$$=\left(\frac{\phi_{i,j+1}-\phi_{ij}}{\Delta y_i}-\frac{\phi_{i-1,j}-\phi_{i-1,j-1}}{\Delta y_{j-1}}\right)^2$$
$$\cdot\left(\frac{\phi_{i+1,j}-\phi_{ij}}{\Delta x_i}-\frac{\phi_{i-1,j}-\phi_{1-2,j}}{\Delta x_{i-2}}\right)^{-2} \tag{14}$$

which is first-order accurate. For shocks with a backward inclination(cf. Fig. 1b), one simply exchanges the index $j+1$ with $j-1$ in Eq. (14). The splitting of the calculation for the ϕ_y-jump into two parts along different vertical lines, as well as the classification of shock inclination, are the essential ingredients in the procedure, which ensures the shock to be treated as one with a slope discontinuity on the potential surface. The original difference equation for upstream point Q (on the same vertical) must also be implemented for the inclination types 1) and 2), because one of the five points in the backward (upwind) hyperbolic operator for Q has been lost to the other side of the shock. The needed datum is supplied by extrapolation to P from three upstream points.

2) *Shock with Supersonic Downstream*

If the flow right behind the shock is supersonic, not only point P [and point Q, in cases 1 and 3 of Fig. 1] but also the downstream point S require special treatment with regard to their difference equation. Unlike the preceding case, Eq. (14), with each i change to $i-1$, is used to determine the ϕ value at the (first downstream) point S. This is because the hyperbolic operator requires one more upstream grid point than the elliptic one does, and also because application of Eq. (14) to determine ϕ and P (right behind the shock) would contradict with the rule of forbidden signals! The (new) ϕ-value at P is determined (in each iteration) by extrapolation along the vertical from a point above [in the case of 1] or below [in the case of 2]. At this latter neighboring point, ϕ is computed from Eq. (14) if the point happens to be an S point on the next horizontal line, and by extrapolation along the vertical, otherwise. The upstream hyperbolic point Q is treated in the same manner as in the case with a subsonic downstream.

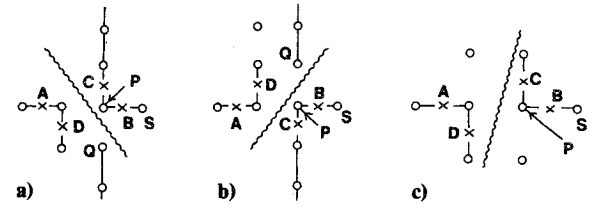

Fig. 1 Grid-point arrangements and three types of shock inclinations to be distinguished in the present shock-fitting method.

**Eq. (12) is fully conservative only for a uniform grid and is, otherwise, conservative to the first-order in Δ.

The application of the (regular) hyperbolic difference operator downstream of P begins with the third points downstream from it, such as point K in Fig. 2. If the shock is sufficiently oblique, or the mesh size Δy is too large, the shock inclination may be such as to exclude the point directly above K from the downstream-flow region. To apply the hyperbolic operator at K in this instance requires another implementation via analytic continuation along the vertical. Here, we express the ϕ value at the shock in terms of ϕ's at the upstream grid points, from which the proper value at the point above K (representing the analytic continuation of ϕ surface from the downstream side) can be determined. Obviously, the occurrence of the various shock inclinations in the supersonic downstream case, and the required implementations, depend on the relative magnitude of the shock slope $(dx^D/dy)^{-1}$ and the mesh ratio $\Delta y/\Delta x$ More extrapolation works along the vertical are needed if the shock becomes more inclined.

If the mesh Δy is small enough, or the Δx is large enough, one may find a rare but possible situation similar to 3 of Fig. 1 to occur for the (present) case involving a supersonic downstream. This has not been taken into account in the present program, and its treatment would entail extra programming work involving extrapolation along the vertical and along the shock.

B. The Modified Line Relaxation Procedure

The foregoing treatments for the shock and neighboring points, together with the hyperbolic, elliptic, parabolic, and the boundary-difference operators applied to other points, complete the difference-equation system. In the line-relaxation procedure, the line of constant x is swept from the upstream to the downstream, with the relaxation factor 1.9 for $U_{ij}>0$, and 0.9 for $U_{ij}<0$. At the shock point P where the flow is subsonic, the difference form of the shock condition, Eq. (14), is applied with data at upstream points known from the most recent sweep, and that at the downstream point S, i.e., $\phi_{i+1,j}$, as well as those on the right-hand side of Eq. (14), are taken from the previous iteration. If the flow right behind the shock is supersonic, Eq. (14), with i changes to $i-1$, is used at point S downstream of P as mentioned earlier; data pertaining to the upstream points of S as well as those on the right-hand side of Eq. (14) are taken either from the most recent sweep or from the previous iteration. In either case, it leads to two (linearized) tridiagonal matrix equations for the line above and below the shock, which can be readily inverted.

For a purely supersonic flow region, a single-sweep procedure *marching forward* in x can be used. The algorithm to treat the supersonic-supersonic transition remains basically the same as in the iterative procedure, except that the shock inclination is determined from the difference form of Eq. (4) prior to the application of Eq. (14) at the next vertical line (downstream). Since Eq. (14) is cubic for the unknown at point S, an inner iterative loop is needed for this single-sweep procedure.

C. Relocating the Shock and Sonic Boundaries

The sonic and shock boundaries are relocated at the end of each step using updated values of ϕ. This step is important for a consistent treatment of the elliptic and hyperbolic points.

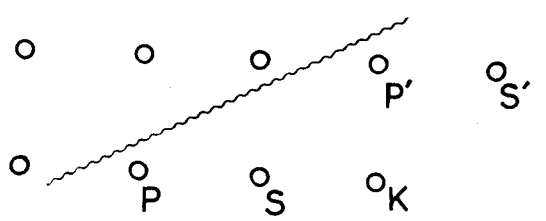

Fig. 2 Grid-point arrangement in application of shock-fitting to a supersonic-supersonic transition.

The sonic boundary is identified with the transition point $U_{ij}=0$ (cf. definition of U_{ij} (in Sec. II, C.), as in Refs. 6, 7, 12, and 13. The shock position is relocated by the intersection of the (new) ϕ-surfaces extrapolated from data obtained for the recent sweep, invoking, once again, the continuity of ϕ.

The initial input (guess) for this iterative solution must include (the location of) the shock boundary. In the course of the iteration, a shock, which was incorrectly assumed at the start, will be deplaced, strengthened, weakened or reduced to a negligible strength. A criterion is used to distinguish the shock from an isentropic compression in making the initial guess for the shock boundary. A point with the flow deceleration from a supersonic speed and a decelerating rate ϕ_{xx} greater than a certain positive number, i.e.

$$K_c-(\gamma+1)\phi_x<0 \quad \text{and} \quad -\phi_{xx}>m>0 \tag{15}$$

is to be taken as a shock point, at which Eq. (14) will then be applied in the subsequent iteration. One needs a large enough m to filter out the smooth recompression waves from the shock. We find the choice of $m=5$ suffices in most of our analyses. A smaller m would allow more shocks in the initial guess (leading, perhaps, to more unwarranted computing works) but is necessary in treating very weak shocks or shocks with a supersonic downstream, for which $-\phi_{xx}$ so computed may not be as large as 5.

D. Local Grid Refinement

Shock-fitting permits the use of a grid coarser than those required for shock-capturing for the same accuracy. However, if the shock is terminated at a solid surface, the coarser grid must still be sufficiently refined near the shock root owing to the re-expansion singularity noted earlier. However, a solution with a finer grid needs to be carried out only in a smaller domain enclosing the shock, with boundary value of ϕ taken from the solution for the coarser grid. This localized grid refinement may thus be made without increasing the dimension of the iterative matrix. In practice, one application suffices (cf. Sec. IV; successive application of the grid refinement is not required). For SPO solution, we found such a grid refinement procedure is also necessary.

E. Relation to SPO

In passing, we observe that the line-relaxation procedure with shock fitting reduces to essentially that with SPO, wherever the shock is normal. In this instance, the right-hand side of Eq. (14) vanishes and the special treatment of the neighboring point Q also becomes unnecessary (Sec. III.A.1). In fact, if one were to enforce a normal shock jump at all shock points, by switching off the right-hand side of Eq. (14), irrespective of the shock inclinations, the shock-fitting solution should reproduce very closely the SPO solution (at least for the case with a subsonic downstream). Several cases of shock-fitting solutions using the normal shock jump described above (referred to in Ref. 13 as NSF solutions) have been made in the course of the study; the results, indeed, compare closely to those with the SPO.††

IV. Application and Discussion

A. Line Relaxation Programs with Shock Fittings and with SPO

Since certain details in the computer programs are not identical, a direct comparison of our shock-fitting solution with Murman's "FCR" data given in Ref. 7 may not bring out conclusively the difference of shock-fitting and shock-capturing (with SPO). A line-relaxation program with SPO was, therefore, written for the present study, and, except for the departure owing to the difference shock treatments, is

††In this respect, the present procedure could be viewed as a modification of one with SPO. Their relation is further delineated in the Appendix.

very much the same as the program used for shock-fitting (including the grid-refinement). Comparison of difference solutions by the two methods is made for the same grid. For convenience, relaxation solutions with shock-fitting will be referred to below simply as "shock-fitting solutions," and those capturing shock with SPO simply as "SPO solutions." Solutions generated from the equivalent of Murman and Cole[6] without specific shock treatment will be designated as "shock-capturing without SPO."

The specific problems analyzed are transonic flows past thin symmetric parabolic-arc airfoils. One problem has a (high) subsonic freestream with $K_c = 1.8$, the other has a (low) supersonic freestream with $K_c = -1.829$. The subsonic example involves an imbedded supersonic region with a shock boundary terminated at the airfoil surface; to describe satisfactorily the shock jump and the flow behavior associated with the re-expansion singularity, a fine grid around the shock is required in this case (cf. Sec. III. D.). However, the finest meshes employed here for shock-fitting solutions are still very much larger than that required for SPO solutions for the same accuracy (see Sec. IV. B.). Shock-fitting solution such as the supersonic example considered in Sec. IV. C., in which shocks do not terminate at airfoil (or wall) surfaces, are much easier and less costly to perform.

B. An Example with an Imbedded Shock

The solutions generated from the basic relaxation program provide the initial (trial) solution, and, for the case with $K_c = 1.8$, it also indicates a supercritical-flow region with a shock near the three-quarter-chord point.

1) Mesh Sizes and Computation Work

A variable grid, with the finest meshes typically $\Delta x = 0.0125$ and $\Delta y = 0.01333$ next to the airfoil, is applied over a small rectangular region $0 < x < 1$, $0 < y < 0.59$ enclosing the shock, in a manner described in Sec. III. D. The total number of grid points corresponding to the unknown has been kept at 81×31, the same as in our basic relaxation program. The same grid is used in the shock-fitting solutions as well as the SPO solutions.‡‡ Iterative solutions for both solution procedures converges satisfactorily in 100-200 iterations. The additional computer time, per iteration, needed for shock-fitting in no case exceeds 5% of the amount normally required for shock-capturing. (The total computer time for an adequately converged solution is close to five (5) minutes on an IBM 370/158 for either procedure.)

We note in passing that the finest mesh mentioned above is still much coarser than the uniform grid used by Murman for establishing accuracy in his SPO solution in Ref. 7, of which $\Delta x = 0.002$ (500 points over a half chord) and $\Delta y = 0.008$.

2) Comparison with Shock Polar

A critical test of the methods in question is to compare the shock jumps in their solutions with the hodograph shock polar. This can be carried out conveniently in the shock jump variables $\hat{u}$ and $\hat{v}$ of Eq. (5) and (6), which permit a study of shock jumps for the entire field in a single graph. To demonstrate the improvement over SPO through shock-fitting, we examine the SPO solution and the shock-fitting solution obtained for the *same* grid.

To define the shock jumps of the SPO solutions for the present purpose, we rely on the fact that ϕ_x distributions (at a fixed y) upstream and downstream of the shock are distinguishable from the smeared-out solution pertaining to the transition zone. As one moves downstream at a fixed y, the first supersonic grid point where ϕ_{xx} undergoes substantial change is taken as the preshock point, to which the preshock values are referred. The point where the trend of the downstream flow begins to establish, is taken to be the post-shock point, to which the post-shock values are referred. These two points, hence, the shock jumps, are readily identified in the plots of ϕ_x and ϕ_y vs x (at a fixed y). For the shock-fitting solution, the jumps are deduced from the stored data of the final solution (using second-order accurate formulae in the extrapolation work).§§

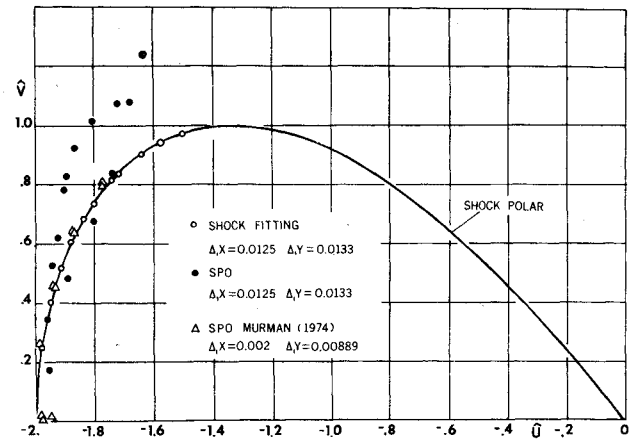

Fig. 3 Comparison of shock jumps determined from shock-fitting and SPO solutions in the hodograph plane. (An imbedded shock over a parabolic-arc airfoil at $K_c = 1.8$.)

The jumps in the SPO and shock-fitting solutions determined in the above manner are correlated as $\hat{v}$ vs $\hat{u}$ in Fig. 3 where the shock polar of Eq. (6) is also shown. The SPO solution obtained with the smallest meshes $\Delta_1 x = 0.0125$, $\Delta_1 y = 0.0133$ are presented as filled circular dots for different locations along the shock. The departure of the dots from the polar curve indicates clearly that, for the mesh sizes employed, the SPO is not effective in describing the more oblique part of the shock. On the other hand, the corresponding shock-fitting solution using the same grid (presented in open circles) is in good agreement with the shock polar.

Included also in Fig. 3 are the shock jump deduced from the SPO solution computed by Murman[7] which are presented in the open triangles and compare reasonably well with the polar curve. These data obtained from Ref. 7 with meshes much finer than those used here ($\Delta x = 0.002$) confirm that the oblique shock relation can be satisfied through SPO, if the grid is made very fine.

With few exceptions, SPO solutions take *four* or more grid points to make the transition from a supersonic to a subsonic flow, irrespective of mesh sizes.[7,13] This has been made apparent in Ref. 7 by the hodograph representation of the solutions at various (fixed) y, in a form similar to the correlations of Fig. 3 (see Fig. 11a of Ref. 13).

An extrapolation of the recorded shock data indicates that the post-shock Mach number becomes unity at $y = 0.20 - 0.225$, and that the shock strength vanishes at a point slightly beyond $y = 0.23 - 0.25$. These suggest that the sonic boundary intersects the imbedded shock from behind. Thus, the flow region behind the shock above the intersection is supersonic. This region is, however, too narrow (about two x-meshes) to allow the use of shock-fitting along with the hyperbolic difference operator described in Sec. III. A.2.

3) Surface Pressure

Figure 4 provides a comparison of shock-fitting and shock-capturing solutions for the ϕ_x-distribution at $0.2 < x < 1.0$ and $y = 0$, corresponding to the surface pressure over the rear half of the airfoil. The two most important solutions in this comparison are the solid curve representing shock-fitting and the dash curve representing SPO, obtained for the same grid

‡‡In fact, an accurate SPO solution requires a grid finer than the one employed here. In other words, SPO cannot fully succeed without grid refinement.

§§Other procedures of defining shock jump from SPO solutions have been tried, with results showing no substantial differences.

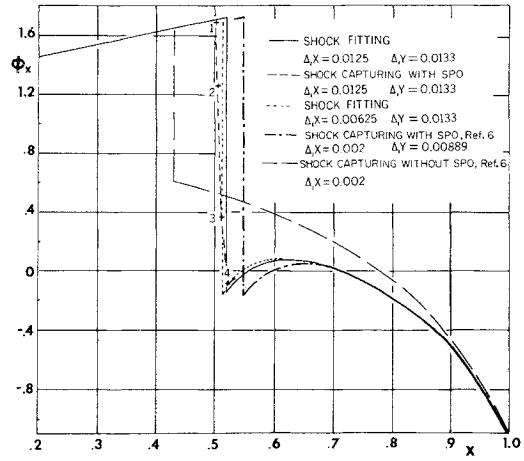

Fig. 4 Comparison of surface velocity determined from shock-fitting and SPO (parabolic-arc airfoil at $K_c = 1.8$).

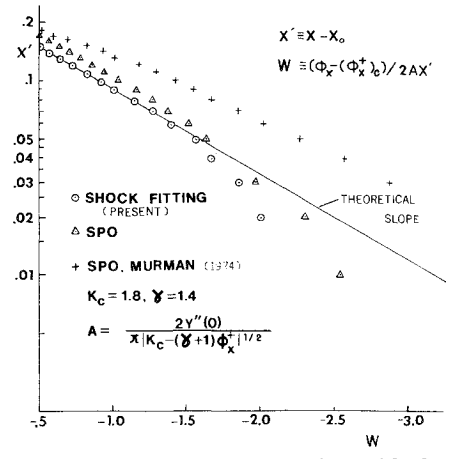

Fig. 5 Correlation of surface velocity data with the re-expansion singularity.

($\Delta_1 x = 0.0125$, $\Delta_1 y = 0.0133$). Except for the spread of the shock transition (marked by points, 1, 2, 3, and 4) and for a rather small reduction in shock jump, the SPO differs little from the shock-fitting. The agreement is not surprising, since appreciable difference between the two in the preceeding figure occur mainly for points removed from the axis of the shock polar.

A shock-fitting solution with an x-mesh half as small ($\Delta_1 x = 0.00625$) is included as a dotted curve and the difference resulting from grid halving is noticeable, but rather small. The corresponding data taken from SPO solution obtained earlier by Murman in Ref. 7 are reproduced here as a dash-dot curve; it gives a distribution slightly, but noticeably different from the preceding three generated in the present study. These differences (1.5% in shock location and 2% in shock strength) cannot be taken to be very significant, inasmuch as program details in our SPO solution and those of Ref. 7 may differ considerably. We shall examine more closely the possible sources of the discrepancies later.

Shock-fitting, as well as SPO, solutions presented in Fig. 4 all satisfy the jump condition next to a wall [Eq. (7)] adequately. [The theoretical mean value of ϕ_x in this case is $K_c/(\gamma+1) = 0.75$.] They represent a substantial improvement over the original shock-capturing solution of Murman and Cole[6] which fails to produce the correct jump even with exceedingly fine meshes. To illustrate this point, the Murman and Cole solution (without SPO) for a very fine mesh ($\Delta x = 0.002$) is reproduced here from Ref. 7 as a thin lone dash curve.

Murman's SPO results and those obtained for the present study agree in the range *beyond* $0.5 < x < 0.7$ (Fig. 4). This suggests that the farfield representation used in the two works is not the source of the discrepancy noted earlier. If the grid used in the grid-refinement were too narrow, its upstream boundary may touch the upper end of a forward-inclined shock, and consequently displace it. This does not appear to happen in our own calculations since the change resulting from using two fine grids of different sizes has been shown to be rather small. It is also believed that our results are sufficiently close to convergence limits; in most of our solutions, one hundred-twenty iterations were used with changes in ϕ_x (next to the shock) less than 10^{-3} per 20 iterations at the end of the run.¶¶

4) *Re-Expansion Singularity*

Another test of the adequacy of our numerical solutions can be made on the basis of their ability to reproduce the Oswatitsch-Zierep singularity. As noted in Sec. II B., the singularity arises from a mismatch of the surface streamline curvature with that determined by the hodograph shock polar; as such, it represents an interaction of the subsonic flow and the shock.

In Fig. 5, the surface velocity from the shock-fitting solution (in open circles) is correlated as

$$(x - x_0) \text{ vs } (\phi_x - (\phi_x^+)_0)/4\pi^{-1}|(\gamma+1)^{-1}[\![\phi_x]\!]_0|^{-\frac{1}{2}} Y''(x)$$

which is equivalent to Eq. (9) at $y = 0$. On a semilogarithmic graph paper with the base ten, the curve is a straight line with a slope of ℓn (10), according to Eq. (9). Except for the first three grid points, the data reproduce the theoretical slope very well, these include the maximum velocity point, as well as portions of the accelerating and decelerating ranges. The discrepancy for the first few grid points is not unexpected, since the truncation error there has been estimated (Sec. II B.) to be of the order $\Delta_1 x \ell n\,(x - x_0)$. Similar correlations applied to data from our SPO program (in triangular symbols) gives essentially the same result except for a minor shift. Thus, the examination has added credence to both our shock-fitting and SPO solution data. SPO data taken from Ref. 7 (in cross symbols), also has the same trend but does not correlate with the theoretical slope as satisfactory as those in circles and triangles.

C. An Example with a Detached Bow Shock

The problem with a bow shock provides a test case for shock-fitting devoid of the re-expansion singularity. Computation work is greatly reduced in this case not only because the mesh sizes may now be made larger and grid refinement is unnecessary, but because the elliptic regions bounded by the bow shock and the sonic boundary can be analyzed, independently of the supersonic flow downstream (of the limiting characteristics). For the latter flow region, a single-sweep shock-fitting procedure [Sec. III A2)] is used.

The particular problem studied is one of a parabolic-arc airfoil in a slightly supersonic stream with a transonic parameter $K_c = -1.829$. Following Murman and Cole,[6] we take K_c to be $(1 - M_\infty^2)/M_\infty \tau^{2/3}$, and this corresponds to the flow past a 6% parabolic arc with $M_\infty = 1.15$. The latter has been analyzed by Magnus,[4] using a time-dependent (diffusive two-step, Lax-Wendroff) method. Application of shock-fitting is further simplifed by the fact that the flow is uniform upstream of the shock ($\phi \equiv 0$), this also eliminates the need for a farfield description. For the calculation, we use a uniform grid $\Delta x = 0.05$ and $\Delta y = 0.10$, considerably coarser than those used in Sec. IV.B. With $\phi = 0$ everywhere as an initial guess, the solution of Magnus[4] is recovered (to within 1% in ϕ_x) in 240 iterations. Figure 6 presents the results for the bow shock (in open circles) and the sonic boundary (in dots) recovered

¶¶We suggest that the small discrepancy with Murman's data is due, perhaps, to too narrow a grid used for grid refinement in Ref. 7.

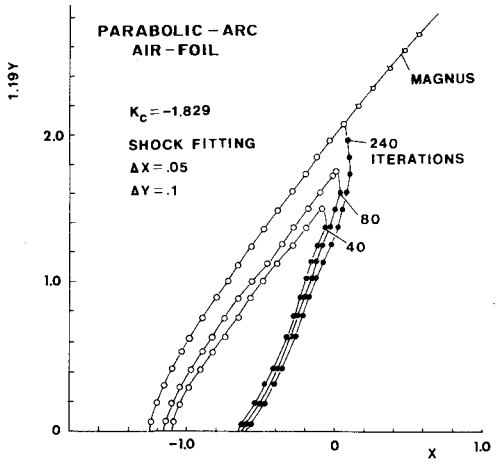

Fig. 6 Comparison of bow shocks and sonic boundaries determined from shock-fitting relaxation solution and time-dependent shock-capturing method (parabolic-arc airfoil at $K_c = -1.829$, uniform grid $\Delta x = 0.05$, $\Delta y = 0.10$).

from the stored solution data. The open circles with slashes are data generated from a single sweep. The rather close agreement with Marnus solution must be considered as being surprising since our shock-fitting scheme is only first-order accurate. The bow shock captured by our corresponding SPO solution (not shown) compares also quite well with Magnus' result, as already demonstrated by Murman.[7] However, the success of the SPO solution in this case depends to a certain degree on a suitable definition of the shock boundary, since a SPO solution normally takes 5-8 grid points to complete a supersonic-supersonic shock transition (cf. Fig. 3 of Ref. 7). Shock-fitting gives more definitive resolution in the shock location and in the pressure signature, and is, therefore, more suited for sonic-boom and caustic analyses.

Line relaxation with shock-fitting can also be accelerated, applying nonlinear transformations cyclically. With the acceleration technique based on the second-order transform,[12,13] we have succeeded in recovering the same bow shock solution (to within 1%) in 64 iterations.

V. Conclusions

A shock-fitting scheme implementing the line-relaxation solution to the transonic small-disturbance equation has been developed. The difference algorithm treats the shock as a discontinuity surface and distinguishes a supersonic downstream flow from a subsonic one; its implementation is consistent with the type-sensitive difference schemes and with the rule of forbidden signals.

Examples testing the procedure include supercritical flows involving an imbedded shock as well as one with a bow shock. Accuracy of the solutions is demonstrated through correlation with the shock polar and with the Oswatitsch and Zierep singularity. Except for a slight but noticeable difference from the surface velocity data of Ref. 7 (discussed in the last section), the shock-fitting solution agrees quite well with Magnus'[4] time-dependent (shock capturing) calculation and with Murman's[7] SPO (shock-capturing) solution which employs an exceedingly fine grid.

Whereas, shock-capturing with SPO is relatively simple to use, it requires a very fine grid and works poorly wherever the post-shock flow is supersonic. The program using shock-fitting is, of course, more complex, but the computing work per sweep proves to differ little from that for the SPO program. Unless the grid could be indefinitely refined, there is a definite improvement by the shock-fitting over the SPO in determining the shock jump and in locating the shock boundary, as has been demonstrated here for the same grid. For a given accuracy level, the shock-fitting scheme certainly represents a greater savings in the computer time.

We may recall that a fine grid is needed around the shock mainly because of the re-expansion singularity at the shock root. With this local grid refinement, the computing time to converge a shock-fitting solution is about the same as that required by the basic shock-capturing program which generates the initial (trial) data. Because of the poorer accuracy, the SPO program will need a finer grid, and therefore a longer computing time. For a problem in which the shock does not terminate on a solid surface, the shock-fitting solution can be obtained with a relatively coarse grid, as the comparison with Magnus' solution has confirmed.

An acceleration technique based on the power method has been applied to the relaxation solution with shock-fitting.[12,13] Savings in the number of iterations and in computer time by a factor of four has been demonstrated.

The present shock-fitting method may be extended and applied to the fully nonlinear potential flow as well as the analyses based on finite-element methods. The procedure should prove useful to perturbation analyses of steady or unsteady potential flows involving shock waves.

Appendix

SPO and Shock Fitting

While Murman derived his scheme based on *global* considerations (satisfying conservation laws), one may examine the shock-point operator (when the flow downstream of the shock is subsnoic) near the shock-point, comparing the shock-point operator to the shock-jump relation. Thus, if we envision a locally normal shock between i and $i-1$, the transonic small-disturbance shock polar equation reduces to Eq. (7) in the text

$$\langle K_c - (\gamma+1)\phi_x \rangle = 0$$

or,

$$2K_c/(\gamma+1) - [(\phi_x)^+ + (\phi_x)^-] = 0 \tag{A1}$$

If we consider $[(\phi_{i-1} - \phi_{i-2})/\Delta x$ as a first-order approximation to ϕ_x^-, then

$$\phi_x^+ = 2K_c/(\gamma+1) - (\Delta x)^{-1}(\phi_{i-1} - \phi_{i-2})$$

$$= 2K_c/(\gamma+1) - (\phi_x)_{i-3/2} \tag{A2}$$

At the grid point i, where the flow is subsonic, a finite-difference approximation of the elliptic equation which considers the shock as an (internal) boundary is

$$\left\{K_c - \frac{\gamma+1}{2}\left[(\phi_x)_{i+1/2} + \phi_x^+\right]\right\}\left\{\Delta x^{-1}\left[(\phi_x)_{i+1/2} - \phi_x^+\right]\right\}$$

$$+ \{\phi_{yy}\}_{CD} = 0 \tag{A3}$$

where the subscript "CD" refers to the central difference. Substituting Eqs. (A2) in (A3) yields, for a uniform grid,

$$\left\{K_c - \frac{\gamma+1}{2}\left[(\phi_x)_{i+1/2} + (\phi_x)_{i-3/2}\right]\right\}$$

$$\times\left\{\Delta^{-1}\left[(\phi_x)_{i+1/2} - (\phi_x)_{i-3/2}\right]\right\} + \{\phi_{yy}\}_{CD} = 0$$

This relation is exactly the same as the SPO given by Eq. (13). Hence, we conclude that the shock-point operator may be interpreted as an elliptic operator with an upstream boundary condition derivable from a normal shock condition. We observe that, considering ϕ_x^+ as a prescribed boundary value, the difference equation (A3), hence (A4), is first-order accurate. There is, however, an error $O(\Delta x)$ in Eq. (A3) resulting from analytical continuing ϕ_x from right behind the shock to the position $(i-1)$, which is nevertheless acceptable under the first-order accuracy.

Acknowledgments

The study is supported by the Office of Naval Research, Fluid Dynamics Branch, Contract Number N00014-75-C-0520. It is our pleasure to acknowledge the benefit derived from discussions with E. M. Murman and from inputs of the referees.

References

[1]Barnwell, R. D., "Numerical Results for the Diffraction of a Normal Shock Wave by a Sphere for the Subsequent Transient Flow," NASA TR R-268, Sept. 1967.

[2]Grossman, B. and Moretti, G., "Time-dependent Computation of Transonic Flows," AIAA Paper 70-1322, Houston, Texas, 1970.

[3]Moretti, G., "On the Matter of Shock-Fitting," in Proceedings of 4th International Conference on Numerical Methods in Fluid Dynamics," Editor, R. D. Richtmyer, *Lecture Notes in Physics*, Springer-Verlag, 1975.

[4]Magnus, R. M., "The Direct Comparison of the Relaxation Method and the Pseudo-Unsteady Finite Difference Method for Calculating Steady Planar Transonic Flow," General Dynamics, Convair Aerospace Div., San Diego, Calif., TN-73-SP03, 1973.

[5]Yoshihara, H., "Computational Methods for 2D and 3D Transonic Flow with Shocks," AGARD paper reprinted from Lecture Series No. 64 on *Advances in Numerical Fluid Dynamics*, undated.

[6]Murman, E. M. and Cole, J. D., "Calcualtion of Plane Steady Transonic Flow," *AIAA Journal*, Vol. 9, Jan. 1971, pp. 114-121.

[7]Murman, E. M., "Analysis of Embedded Shock Waves Calculated by Relaxation Methods," *AIAA Journal*, Vol. 12, May 1974, pp. 626-633.

[8]Martin, E. D., "A Fast Semidirect Method for Computing Transonic Aerodynamic Flows," *AIAA Journal*, Vol. 14, July 1976, pp. 914-922; errata published in Nov. 1976 issue, p. 1664.

[9]Jameson, A., "Transonic Potential Flow Calculation Using Conservation Form," *Proceedings of the AIAA 2nd Computational Fluid Dynamics Conference*, Hartford, Conn., June 19-20, 1975, pp. 148-161.

[10]Oswatitsch, K. and Zierep, J., "Des Problem des Senkrechten Stossen an Einer Gekrummten Wand," *ZAMM*, Vol. 40, Suppl., 1960, pp. 143-144.

[11]Yu, N. J. and Seebass, R., "Inviscid Transonic Flow Computations with Shock Fitting," *IUTAM Symposium Transonicum II*, Gottingen, 1975, to be published.

[12]Hafez, M. M. and Cheng, H. K., "Convergence Acceleration of Relaxation Solutions for Transonic Flow Computations," *AIAA Journal*, Vol. 15, March 1977, pp. 329-336.

[13]Hafez, M. M. and Cheng, H. K., "Convergence Acceleration and Shock-Fitting for Transonic Aerodynamics Computations," University of Southern California, Los Angeles, Calif., School of Engineering Report *USCAE 132*, April 1975.

[14]Cole, J. D., "Modern Developments in Transonic Flow," *SIAM Journal of Applied Mathematics*, Vol. 29, Dec. 1975, pp. 763-787.

[15]Ackeret, J., Feldman, F., and Rott, N., "Investigation of Compression Shocks and Boundary Layers in Gases Moving at High Speed," *ETH, Zurich Report 10*, 1946, (English translation NACA TM 1113, 1947).

[16]Ferrari, C. and Tricomi, F. G., *Transonic Aerodynamics*, Academic Press, New York, 1968.